Synthesis, crystal structure and INDO calculation of the molecular hyperpolarizability of a highly polarizable merocyanine dye†

Pascal G. Lacroix,* Jean-Claude Daran and Patrick Cassoux

Laboratoire de Chimie de Coordination du CNRS, 205 route de Narbonne, 31077 Toulouse cedex, France

A zwitterionic cyanine dye of formula $HOCH_2CH_2(NC_5H_4)CHCH(C_6H_4)O$ ($\mathbf{M_2}$) is reported with its crystal structure. Crystal data: monoclinic ($P2_1$), $a = 15.038$, $b = 5.385$, $c = 17.301$ Å, $\beta = 111.68$, $Z = 2$. The nonlinear optical properties are investigated through solvatochromism and found to be very similar to those of a related cyanine dye ($\mathbf{M_1}$) having an extremely high molecular hyperpolarizability (β). INDO calculations performed on both crystal structures indicate small modifications in the electronic properties, but which result in a large modification of the hyperpolarizability in the solid: $\beta(\mathbf{M_2}) = 2.5 \times \beta(\mathbf{M_1})$. In addition, the hydroxyethyl substituent can be employed for engineering the chromophore into acentric environments. Therefore, increasing NLO responses may be expected at both the molecular and macroscopic levels with such systems.

Over the last two decades, intense activity in the field of organic synthesis and material engineering has demonstrated the relevance of organic materials for second-order nonlinear optical (NLO) properties.[1–4] In molecular materials, the susceptibility tensor ($\chi^{(2)}$), which determines the second-order response, is related to the underlying molecular hyperpolarizability tensor (β).[5] A large value of β is, therefore, the first prerequisite for high NLO efficiency in a molecular material. The dependence of β on the nature of organic compounds has been extensively explored, both theoretically[6,7] and experimentally,[8] and the search for new NLO molecular structures is still a very active research area.[9] Many efficient chromophores in the 4,4′-disubstituted stilbenes family have been investigated. In this series, the merocyanine dye $\mathbf{M_1}$ (Scheme 1) has the largest β value determined in solution ($\approx 1000 \times 10^{-30}$ cm^5 esu^{-1}).[10] However, this result is based on an approximate dipole moment and is very solvent dependent.[11] In fact, measurements of the molecular NLO response are sometimes questionable, because of the modification of electronic properties caused by environmental interactions. This effect is especially important for the merocyanine dye $\mathbf{M_1}$, which exhibits one of the largest solvatochromic shifts ever reported (*e.g.*, $\lambda_{max} = 620$ nm in chloroform and 442 nm in water).[12–14] The ground state of $\mathbf{M_1}$ can be viewed as a combination of two resonance forms (Scheme 1), both with distinct bond lengths between neighboring carbon atoms. To date, although the crystal structure of $\mathbf{M_1}$ has been published,[15] calculations of the electronic properties were performed on optimized structures only.[16–18] Difficulties encountered in measuring β encourage theoretical investigations of the NLO response based on reliable crystal structures to rationalize the origin and true extent of the properties.

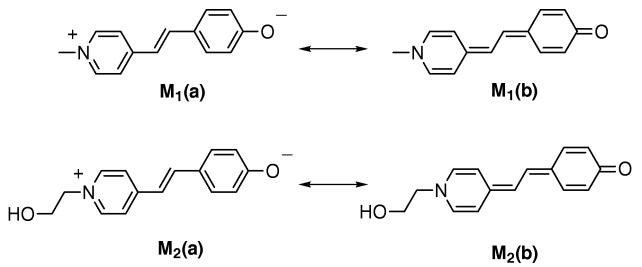

Scheme 1

The present paper reports on 1-(2-hydroxyethyl)-4-(4-hydroxystyryl)pyridinium betaine $\mathbf{M_2}$. Our motivation for studying this molecule was based on the opportunity to provide one more functional substituent (*e.g.*, hydroxy) for further chemical developments on the promising $\mathbf{M_1}$ structure, such as bonding it to a chiral group or a polymer. In addition, the hydroxy group may be used to embody tentatively the chromophores into acentric environments through hydrogen-bonding networks. As our study was in progress, $\mathbf{M_2}$ was briefly reported without synthetic details.[19] Contrary to what is reported in ref. 19(*a*), $\mathbf{M_2}$ is not an amorphous compound. We present here its synthesis and crystal structure. $\mathbf{M_1}$ and $\mathbf{M_2}$ turn out to have similar electronic properties. Their hyperpolarizabilities are investigated in solution (from solvatochromism) and in the solid state (from INDO calculations performed on isolated molecules having the same conformation as in the crystal).

Experimental

Materials and equipment

Starting materials were used as purchased without further purification. UV/VIS spectra were recorded on a Hewlett Packard 8452A spectrophotometer and ^{1}H NMR spectra on a Bruker AM 250 spectrometer. Elemental analysis were performed by the Service de Microanalyses du CNRS Laboratoire de Chimie de Coordination, Toulouse. Thermal measurements were performed by TG/DTA (thermogravimetric/differential thermoanalysis) on a Setaram-TGDTA92 thermoanalyser. The experiments were conducted under nitrogen on 5 mg of sample (heating rate: 10 °C min^{-1}).

Solvents (SDS or Carlo Erba) for the spectroscopic studies were used without further purification. As $\mathbf{M_2}$ is extremely sensitive to traces of acid, it was essential to maintain the solvent basic by addition of a small amount of amine according to the procedure already reported.[12,14]

Synthesis of merocyanine dye $\mathbf{M_2}$ [20]

2-Iodoethanol (3.44 g, 2×10^{-2} mol) was mixed with 10 ml (large excess) of 4-picoline and stirred overnight at room temperature. The excess of picoline was carefully removed under

† Non-SI units employed: 1 esu $\approx 3.33 \times 10^{-10}$ C; 1D $\approx 3.3 \times 10^{-30}$ C m.

vacuum. To the residual yellow oil were successively added 50 ml of 2-propanol, 2.44 g (2×10^{-2} mol) of 4-hydroxybenzaldehyde and 2 ml of piperidine. The resulting red mixture was refluxed for 24 h. After cooling down, a large amount of solid was filtered off, washed with cold 2-propanol and dried under vacuum (90% yield). Red crystals were obtained by recrystallization in an aqueous solution of K_2CO_3 (10^{-1} mol l^{-1}). ^{1}H NMR (DMSO): δ 3.86 (t, 4.9 Hz, 2H), 4.34 (t, 4.6 Hz, 2H), 6.25 (d, 8.6 Hz, 2H), 6.66 (d, 15.8 Hz, 1H), 7.43 (d, 8.8 Hz, 2H), 7.67 (d, 6.4 Hz, 2H), 7.81 (d, 15.2 Hz, 1H), 8.30 (d, 6.5 Hz, 2H). Elemental analysis calcd (found) for $C_{15}H_{15}NO_2 \cdot H_2O$: C, 69.48 (69.5); H, 6.61 (7.2); N, 5.40 (5.3)%. TG analysis indicates a weight loss of 7.097% located at 105 °C, which corresponds to the loss of 1 H_2O per $\mathbf{M_2}$ molecule.

X-Ray structure determination

The data were collected at 160 K on a Stoe Imaging Plate Diffraction System (IPDS) equipped with an Oxford Cryosystems cooler device. The crystal-to-detector distance was 80 mm. One hundred and twenty-five exposures (5 min per exposure) were obtained with $0 < \phi < 200°$ and with the crystals rotated through 1.6° in ϕ. Coverage of the unique set was over 99% complete to at least 24.2°. Crystal decay was monitored by measuring 200 reflections per image. The final unit cell parameters were obtained by the least-squares refinement of 5000 reflections. Only statistical fluctuations were observed in the intensity monitors over the course of the data collection. Owing to the rather low μx value, 0.01, no absorption correction was considered.

The structure was solved by direct methods (SIR92)[21] and refined by least-squares procedures on F_{obs}. H atoms were located on difference Fourier maps, but those attached to C atoms were introduced in the calculation in idealized positions [d(CH) = 0.96 Å] and their atomic coordinates were recalculated after each cycle. They were given isotropic thermal parameters 20% higher than those of the carbon to which they are attached. The coordinates of the H atoms attached to the O atoms were not refined and their isotropic thermal parameters U_{iso} were fixed to 0.08 Å^2. Least-squares refinements were carried out by minimizing the function $\Sigma w(|F_o| - |F_c|)^2$, where F_o and F_c are the observed and calculated structure factors. The weighting scheme used in the last refinement cycles was $w = w'[1 - \Delta F/6\sigma(F_o)^2]^2$ where $w' = 1/\Sigma_1^n A_r T_r(x)$ with 3 A_r coefficients for the Chebyshev polynomial $A_r T_r(x)$, where x was F_c/F_c(max).[22] Models reached convergence with $R = \Sigma(||F_o| - |F_c||)/\Sigma(|F_o|)$ and $Rw = [\Sigma w(|F_o| - |F_c|)^2/\Sigma w(F_o)^2]^{1/2}$ having the values listed in Table 1. Criteria for a satisfactory complete analysis were that the ratio of rms shift to standard deviation be less than 0.1 and that no significant features be present in final difference maps. Details of data collection and refinement are given in Table 1.

The calculations were carried out with the CRYSTALS package of programs[23] running on a PC. The drawing of the molecule was realized with the help of CAMERON.[24]

CCDC reference number 440/055.

Calculation of NLO response of $\mathbf{M_2}$

The all-valence INDO/S (intermediate neglect of differential overlap) method,[25] in connection with the sum-over-states (SOS) formalism,[26] was employed. Details of the computationally efficient INDO-SO-based method for describing second-order molecular optical nonlinearities have been reported elsewhere.[7b] Calculations were performed using the INDO/1 Hamiltonian incorporated in the commercially available MSI software package INSIGHT II (4.0.0). The mono-excited configuration interaction (MECI) approximation was employed to describe the excited states. The 100 energy transitions between the ten highest occupied molecular orbitals and the ten lowest unoccupied ones were chosen to undergo CI mixing. The atomic coordinates used for the calculation were the crystallographic data for $\mathbf{M_1}$[15] and the present data (Table 2, molecule 1) for $\mathbf{M_2}$. No other data were introduced to take into account possible intermolecular interactions in the crystals.

Table 1 Crystal data for $\mathbf{M_2}$

Formula	$(C_{15}H_{15}NO_2)_2$, $2H_2O$
FW/g	518.61
Shape (color)	needle (red)
Size/mm	0.75, 0.13, 0.06
Crystal system	monoclinic
Space group	$P2_1$
a/Å	15.038(2)
b/Å	5.3846(5)
c/Å	17.301(2)
β/°	111.68(1)
U/Å^3	1301.9(3)
Z	2
Temperature/K	160(2)
Radiation	MoKα (λ = 0, 71073)
ρ (calcd)/g cm^{-3}	1.323
μ (MoKα)/cm^{-1}	0.862
$R(F_0)^a$	0.0527
$R_w(F_o)^a$	0.0553
Total reflections	8064
Independent reflections	3972
Reflections used [$I > 2\sigma(I)$]	2011
Refined parameters	334

[a] $R = \Sigma(||F_o| - |F_c||)/\Sigma(|F_o|)$, $Rw = [\Sigma w(|F_o| - |F_c|)^2/\Sigma w(F_o)^2]^{1/2}$.

Results and Discussion

Description of the structure

The molecular structure is shown in Fig. 1 with the atomic numbering scheme employed, while atomic coordinates and selected bond lengths are gathered in Tables 2 and 3, respectively. An intricate hydrogen bonding pattern maintains the cohesion of the crystal. As shown in Fig. 1, the asymmetric unit is built up from two molecules linked by a hydrogen bond. Moreover, there is another H bond between the hydroxyl O1 atom and the O11 of the twofold axis related molecules, resulting in an infinite *zig-zag* chain (Fig. 2). Finally, one of the water molecules, O100, exhibits H interactions with the symmetry-related O21 atoms, whereas the second water molecule, O200, establishes H links between two different chains. Except for the hydroxyethyl groups, $\mathbf{M_2}$ molecules are planar, the largest deviation of −0.083 Å being observed at the C273 atom.

The averaged length of the central C—C bonds (1.316 Å) implies a high double-bond character, while the averaged C—O bond length of 1.295Å is closer to the phenolic length (1.36 Å) than to the C=O double bond value (1.21 Å). These structural data are in agreement with the structure of the related dye $\mathbf{M_1}$[15] (see Table 2) and suggest that the zwitterionic structure **a** (see Scheme 1) is dominant in the ground state of both $\mathbf{M_1}$ and $\mathbf{M_2}$.

Optical spectra of merocyanine $\mathbf{M_2}$

Electronic spectra in methanol are shown in Fig. 3 for $\mathbf{M_1}$ and $\mathbf{M_2}$. It can be seen that both dyes exhibit similar features: same energy transition (E) with λ_{max} recorded at 383 nm ($\mathbf{M_1}$) and 388 nm ($\mathbf{M_2}$) and same oscillator strengths ($f = 0.68$) calculated through the relation[27] $f = 4.315 \times 10^{-9} \int \varepsilon \, d\nu$, where the integration extends over the entire absorption band, ν being the frequency (cm^{-1}).

Electronic spectra of $\mathbf{M_1}$ and $\mathbf{M_2}$ are compared in various

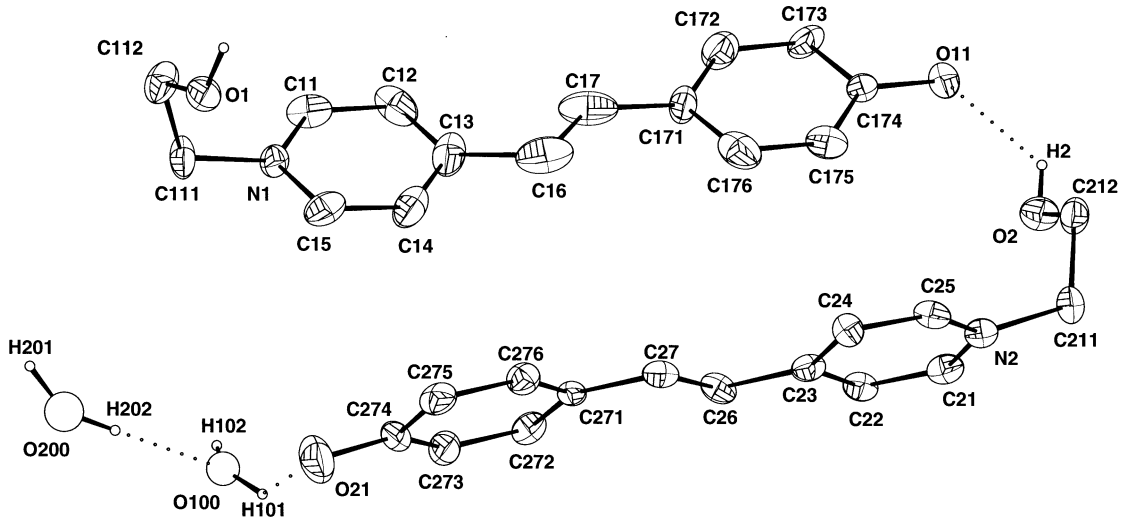

Fig. 1 Unit cell and atom labelling scheme for $\mathbf{M_2}$

solvents in Table 4. It turns out from the examination of these data that both compounds exhibit strong negative solvatochromism (around 140 nm). The solvatochromism of merocyanine dyes is well-known.[28] The origin of this behavior in $\mathbf{M_1}$

Table 2 Fractional atomic coordinates of the non-hydrogen atoms and equivalent isotropic thermal parameter *U*(eq) or isotropic thermal parameter *U*(iso). E.s.d.s in parentheses refer to the last significant digit. *U*(eq) is defined as the cube root of the product of the principal axes

Atom	*x*/*a*	*y*/*b*	*z*/*c*	*U*(eq) or *U*(iso)
Molecule 1				
O1	0.8179(2)	0.7484(6)	0.0867(2)	0.0335
O11	1.0066(2)	0.4050(7)	0.8341(2)	0.0363
N1	0.7460(3)	0.3803(8)	0.1663(2)	0.0249
C11	0.8011(4)	0.203(1)	0.2151(4)	0.0371
C12	0.8297(4)	0.218(1)	0.3007(4)	0.0440
C13	0.7985(4)	0.417(1)	0.3367(3)	0.0417
C14	0.7396(4)	0.590(1)	0.2835(4)	0.0394
C15	0.7151(4)	0.569(1)	0.2008(3)	0.0390
C16	0.8253(4)	0.466(1)	0.4280(5)	0.0553
C17	0.8821(4)	0.324(1)	0.4843(4)	0.0469
C111	0.7261(3)	0.382(1)	0.0757(3)	0.0332
C112	0.8075(4)	0.4982(9)	0.0590(3)	0.0331
C171	0.9120(4)	0.361(1)	0.5759(3)	0.0331
C172	0.9717(4)	0.183(1)	0.6274(4)	0.0398
C173	1.0042(3)	0.195(1)	0.7127(3)	0.0336
C174	0.9771(3)	0.394(1)	0.7535(3)	0.0302
C175	0.9168(4)	0.576(1)	0.7030(3)	0.0331
C176	0.8842(4)	0.562(1)	0.6173(4)	0.0426
O100	0.6051(3)	−0.0869(9)	0.9256(3)	0.068(1)
Molecule 2				
O2	0.8938(2)	0.5791(6)	0.9031(2)	0.0297
O21	0.4495(3)	0.882(1)	0.1466(2)	0.0678
N2	0.7614(3)	0.9508(7)	0.8124(2)	0.0224
C21	0.7045(3)	0.752(1)	0.7824(3)	0.0288
C22	0.6614(3)	0.7128(9)	0.6988(3)	0.0238
C23	0.6763(3)	0.876(1)	0.6412(3)	0.0252
C24	0.7369(3)	1.0798(9)	0.6754(3)	0.0246
C25	0.7770(3)	1.1134(9)	0.7586(3)	0.0257
C26	0.6280(3)	0.8272(9)	0.5521(3)	0.0249
C27	0.6351(3)	0.971(1)	0.4909(3)	0.0268
C211	0.8171(3)	0.9758(9)	0.9028(3)	0.0268
C212	0.9108(4)	0.835(1)	0.9247(3)	0.0316
C271	0.5901(3)	0.934(1)	0.4028(3)	0.0225
C272	0.5312(3)	0.730(1)	0.3661(3)	0.0294
C273	0.4864(3)	0.709(1)	0.2813(3)	0.0336
C274	0.4957(3)	0.892(1)	0.2260(3)	0.0352
C275	0.5581(3)	1.093(1)	0.2632(3)	0.0308
C276	0.6025(3)	1.1143(9)	0.3482(3)	0.0263
O200	0.4163(4)	−0.523(1)	0.9211(3)	0.089(2)

Table 3 Bond lengths (Å) for $\mathbf{M_1}$ and $\mathbf{M_2}$. E.s.d.s in parentheses refer to the last significant digit. Data for $\mathbf{M_1}$ are from ref. 15 and atoms for $\mathbf{M_2}$ are labelled as for $\mathbf{M_1}$, to make comparisons possible

$\mathbf{M_2}$			
O1—C112	1.419(6)	O2—C212	1.428(6)
O11—C174	1.298(6)	O21—C274	1.292(6)
N1—C11	1.338(7)	N2—C21	1.348(6)
N1—C15	1.346(7)	N2—C25	1.361(6)
N1—C111	1.483(6)	N2—C211	1.482(6)
C11—C12	1.383(8)	C21—C22	1.365(7)
C12—C13	1.404(9)	C22—C23	1.410(7)
C13—C14	1.378(8)	C23—C24	1.408(7)
C13—C16	1.503(9)	C23—C26	1.464(7)
C14—C15	1.345(8)	C24—C25	1.351(7)
C16—C17	1.285(8)	C26—C27	1.348(7)
C17—C171	1.494(8)	C27—C271	1.433(6)
C111—C112	1.495(7)	C211—C212	1.518(7)
C171—C172	1.387(8)	C271—C272	1.408(7)
C171—C176	1.442(8)	C271—C276	1.412(7)
C172—C173	1.373(8)	C272—C273	1.374(7)
C173—C174	1.421(7)	C273—C274	1.417(8)
C174—C175	1.404(8)	C274—C275	1.420(8)
C175—C176	1.381(8)	C275—C276	1.377(7)
$\mathbf{M_1}$			
O11—C174	1.304(3)	C16—C17	1.346(4)
N1—C11	1.353(3)	C17—C171	1.439(3)
N1—C15	1.347(4)	C171—C172	1.408(4)
N1—C111	1.479(3)	C171—C176	1.404(4)
C11—C12	1.359(4)	C172—C173	1.379(4)
C12—C13	1.405(4)	C173—C174	1.414(4)
C13—C14	1.497(4)	C174—C175	1.421(4)
C13—C16	1.441(4)	C175—C176	1.404(4)
C14—C15	1.361(4)		

Table 4 Absorption maxima of the lowest energy optical transition for merocyanine $\mathbf{M_1}$ (taken from ref. 13) and $\mathbf{M_2}$ in solvents of different polarities

Solvent	λ_{max}/nm $\mathbf{M_1}$	λ_{max}/nm $\mathbf{M_2}$
Water	442	448
Methanol	483	488
2-Propanol	545	548
Acetonitrile	571	571
DMF	582	584
Acetone	585	586

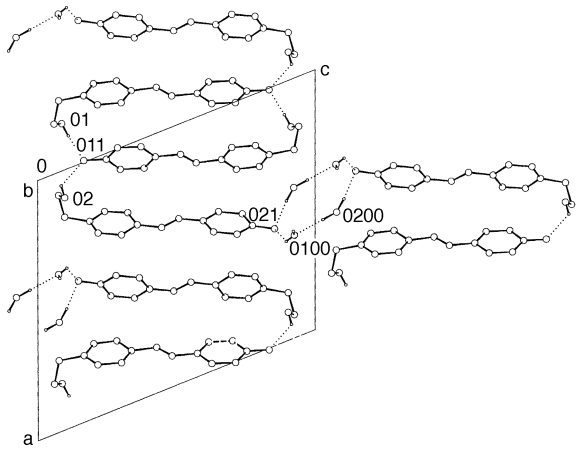

Fig. 2 $\mathbf{M_2}$ stacking and hydrogen-bonded network structure for $\mathbf{M_2}$

is still controversial. It was recently suggested that the solvatochromic shift is not due to the dipolarity-polarizability of the solvent but to its hydrogen-bond donor acidity.[12] In addition, an inverted solvatochromism at low polarity has been observed in $\mathbf{M_1}$ and attributed to a change in the molecular structure with a stabilization of the nonionic $\mathbf{M_1(b)}$ form.[14] Various studies were conducted to rationalize the solvation effect in relation to changes in geometry using semiempirical CNDO calculations[16] or within the COSMO model.[17] Adequate treatment of solvation effects in the UV/VIS spectra is a complicated task and a general solution of this problem is not the purpose of the present work.

It may be noted, however, that a negative solvatochromism is usually associated with a decrease of the dipole moment upon excitation ($\mu_e < \mu_g$), due to the stabilization of highly polar forms in the ground state, $\mathbf{M_1(a)}$ and $\mathbf{M_2(a)}$, as anticipated from the crystal structure examination. Large dipole moment changes ($\Delta\mu$) between the ground and the first excited states are, therefore, strongly indicative of large second-order optical nonlinearities (*vide infra*), which has been suggested as a possible method for determining molecular hyperpolarizabilities.[29]

The comparison of the solvatochromic shifts of both dyes is drawn in Fig. 4, as a function of the Reichard solvent parameter (E_T).[30] It can be assumed that $\mathbf{M_1}$ and $\mathbf{M_2}$ exhibit similar molecular shapes, Onsager radii, and dipole moments; therefore, comparing the slopes of the curves in Fig. 4 can amount to comparing $\Delta\mu$.[29] Consequently, the slopes (-237 *vs.* -228) of the curves in Fig. 4 clearly indicate similar $\Delta\mu$ values for both materials. With the relative experimental E, f, and $\Delta\mu$ values of both molecules, and within the framework of the two-level model (*vide infra*), the calculation gives $\beta(\mathbf{M_2}) = 0.99\beta(\mathbf{M_1})$.

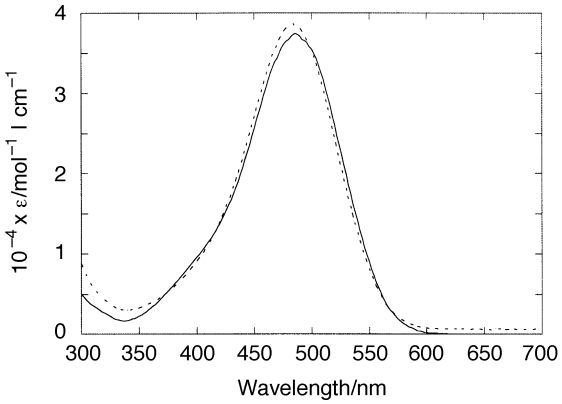

Fig. 3 UV/VIS spectrum $\mathbf{M_2}$ recorded in methanol *versus* that of $\mathbf{M_1}$ (dotted line)

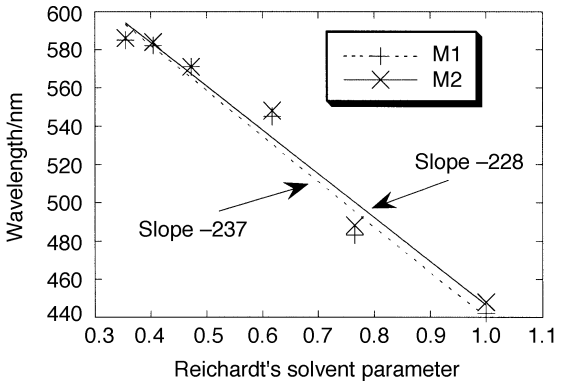

Fig. 4 Solvatochromism of $\mathbf{M_1}$ and $\mathbf{M_2}$ as a function of a solvent parameter. Similar slopes are indicative of similar $\Delta\mu$ values

In conclusion, our measurements allow us to state that the $\mathbf{M_1}$ and $\mathbf{M_2}$ chromophores exhibit similar electronic properties and consequently very closely related optical nonlinearities in solution.

Molecular orbital calculations and NLO response in the solid

The molecular orbital calculations confirm the dominant zwitterionic structure in the ground state of $\mathbf{M_2}$, in agreement with the structure data analysis. The Mulliken population analysis is shown in Fig. 5 for $\mathbf{M_2}$. The phenolate fragment bears a -0.548 charge and is expected to act as a strong donor, while the pyridinium is the acceptor counterpart. This important charge delocalization results in a calculated ground state dipole moment of 27.6 D.

The calculated second-order hyperpolarizability of $\mathbf{M_2}$ is shown in Table 5 and compared to that of $\mathbf{M_1}$, based on the published structure.[15] Before comparing the results, it must be remembered that two molecules are present in the asymmetric unit cell of $\mathbf{M_2}$. The calculations presented in this study are those performed on molecule 1 (Table 2). However, the electronic properties of molecule 2 show the same general trend as molecule 1 *versus* the parent $\mathbf{M_1}$ dye, however, to a lesser extent. The calculation is performed at 1.907 μm and at zero frequency. [Experiments conducted with a laser operating at 1.064 μm would be of no use for second-order NLO applications, because of the absorption of the second harmonic frequency (532 nm) by the chromophores.] Within the framework

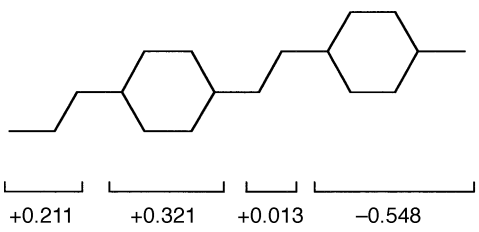

Fig. 5 Mulliken population analysis for $\mathbf{M_2}$

Table 5 Molecular hyperpolarizability (β) calculated at different laser frequencies for $\mathbf{M_1}$ and $\mathbf{M_2}$

	β 10^{-30} cm^5 esu^{-1}			
	$\mathbf{M_1}$		$\mathbf{M_2}$	
λ/μm	β_{tot}	$\beta_{2\text{-level}}$	β_{tot}	$\beta_{2\text{-level}}$
∞	196	270	431	575
1.907	317	414	829	1036

of SOS perturbation theory, the molecular hyperpolarizability can be related to all excited states of the molecule and can be partitioned into two contributions, so-called two-level and three-level terms.[31] Analysis of term contributions to the molecular hyperpolarizability of $\mathbf{M_1}$ and $\mathbf{M_2}$ (Table 5) indicates that two-level terms dominate the nonlinearity, which, as explained below, can be related to a single low-lying electronic transition. What is immediately striking when the β of $\mathbf{M_1}$ and $\mathbf{M_2}$ are compared is the disagreement between calculations and experimental spectra. Table 4 and Figs. 3 and 4 are strongly indicative of closely related hyperpolarizabilities in solution. In contrast to these observations, the calculated β values are roughly 2.5 times higher for $\mathbf{M_2}$ than for $\mathbf{M_1}$. This important difference, at first surprising, can tentatively be discussed by considering the possibility of equilibria between resonant structures (Scheme 1), associated with different geometrical features. The solvent effects on the hyperpolarazability of the NLO chromophore are already well-known.[32–34] Therefore, it is understandable that slight modifications of the environment (*e.g.*, effect of crystal packing) may result in slight modifications of the molecular geometry, thus accounting for large differences in the electronic properties in the solid state, as they account for differences observed between NLO experiments carried out in different solvents. These last few years, the effect of intermolecular interactions on the hyperpolarizability has been theoretically investigated and found to be important in some cases.[35] In the present study, the calculations were performed on isolated molecules and possible intermolecular interactions were not taken into account, except by using the experimental geometry in the calculation. Eventually, it has to be remembered that the electronic hyperpolarizability (this work) is not the only origin of the total NLO response, which also implies a vibronic component.[36] Vibronic hyperpolarizability, which has received limited attention in the past, has not been taken into account in the present paper. However, a recent review has pointed out its importance for donor-acceptor conjugated systems.[36]

According to the well-known and widely used two-level model,[37] it has long been recognized that the longest wavelength absorption band of disubstituted benzene derivatives is responsible for the second-order NLO response of the molecule. In this model, the hyperpolarizability (β) can be described in terms of a ground and a first excited state, which has charge transfer character, and is related to the energy of the optical transition (E), its oscillator strength (f) and the difference between ground and excited state dipole moments ($\Delta\mu$) through the relation $\beta \propto f \times \Delta\mu/E^3$.

INDO calculated data are reported in Table 6 for the low-lying transitions of $\mathbf{M_1}$ and $\mathbf{M_2}$. In good agreement with the electronic spectra, this calculation shows that both dyes exhibit only one intense low-lying optical transition (large oscillator strength), involving principally the HOMO → LUMO transition. Contrary to the experiment (Table 4, Fig. 3), this transition is red-shifted, with a lower oscillator strength and increasing dipole moment change, upon going from $\mathbf{M_1}$ to $\mathbf{M_2}$. This unexpected effect might tentatively be related to geometrical modifications induced by the environment in the solid state as discussed above.

Atomic orbital contributions to the HOMO and LUMO are shown in Fig. 6 for $\mathbf{M_1}$ and $\mathbf{M_2}$. The intramolecular charge transfer is enhanced in $\mathbf{M_2}$, as indicated by the π electron density on the phenolate and pyridium fragments for the HOMO and LUMO, respectively. In a previous paper, these orbitals have been calculated within the CNDO/S scheme[16] for $\mathbf{M_1}$ in solution as a function of the environment on the basis of changes in geometries induced by a factor, $f(\varepsilon)$, which defines the solvent polarity as $f(\varepsilon) = 1 - (1/\varepsilon^{1/2})$, where ε is the dielectric constant of the solvent. With the assumption of a small interaction factor, $f(\varepsilon) \approx 0$, it turns out that both results are qualitatively similar. In the present study, the HOMO and LUMO obtained for $\mathbf{M_1}$ and $\mathbf{M_2}$, on the basis of experimental geometries, are equal to what is calculated with an interaction factor, corresponding to a situation of higher polarity for $\mathbf{M_2}$ than that encountered for $\mathbf{M_1}$. In any case, the results of the calculations are strongly dependent on subtle changes in geometry due to different packings, upon going from $\mathbf{M_1}$ to $\mathbf{M_2}$, and cannot be easily explained in terms of polarity differences.

Another property modification occurring from the different crystal structures is related to the centrosymmetry. Contrary to $\mathbf{M_1}$ (centrosymmetric space group $P2_1/c$), $\mathbf{M_2}$ crystallizes in the noncentrosymmetric space group $P2_1$. Therefore, the large molecular hyperpolarizability is expected to give rise in $\mathbf{M_2}$ to an observable bulk susceptibility ($\chi^{(2)}$). However, the angle between β and the two-fold axis (2_1) happens to be close to

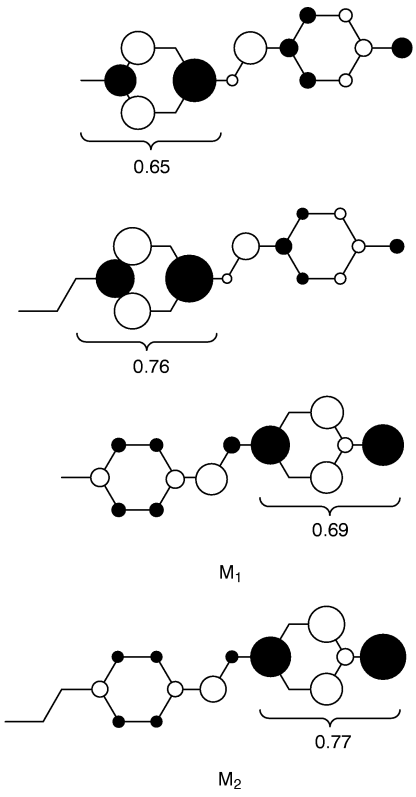

Fig. 6 HOMO (bottom) and LUMO (top) for $\mathbf{M_1}$ and $\mathbf{M_2}$ with the π electron density on selected fragments

Table 6 Energies (λ_{max}), oscillator strengths (f), dipole moment changes between ground and excited state ($\Delta\mu$) and composition of the first excited states of $\mathbf{M_2}$

Compound	Transition	λ_{max}/nm	f	$\Delta\mu$/D	Composition[a] of the CI expansion
$\mathbf{M_1}$	1 → 2	539	2.03	−9.9	$0.965\chi_{40\rightarrow41}$
$\mathbf{M_2}$	1 → 2	613	1.58	−18.2	$0.978\chi_{46\rightarrow47}$

[a] Orbital 40 is the HOMO and orbital 41 is the LUMO in $\mathbf{M_1}$. Orbital 46 is the HOMO and orbital 47 is the LUMO in $\mathbf{M_2}$.

178° for $\mathbf{M_2}$, thus cancelling out most of the nonlinearity by symmetry in the solid state. Consequently, no efficiency was recorded at 1.907 μm (<0.1 times the efficiency of urea in the Kurtz–Perry powder test[38]).

Summary and Conclusion

We have reported on a comparison of the NLO properties of two merocyanine ($\mathbf{M_1}$ and $\mathbf{M_2}$) dyes. From an investigation of the UV/VIS spectra, we have provided strong evidence for optical properties dominated by an intense HOMO → LUMO transition, exhibiting the same features (λ_{max}, f and Δμ), which strongly indicates the same hyperpolarizability for both dyes. In particular, experimental data indicate that the introduction of a hydroxyethyl substituent does not affect the hyperpolarizability of the molecule. On the other hand, calculations performed on the crystal structures show that the hyperpolarizability is very dependent on the molecular environment in the solid state. Further investigations of the modification of β between solid state and solution could require hyperpolarizability measurements by the electric-field-induced second-harmonic (EFISH) technique and calculations of the vibronic hyperpolarizabilities. This latter topic, which has received very limited attention to date, implies the theoretical treatment of the action of external electric fields on the vibrational degrees of freedom of the chromophore. Clearly, we are just beginning to learn about the quantitative role of the medium in determining NLO properties in the solid state. Such calculations could be helpful to rationalize the effect of vibrational motion on the NLO properties in the solid.

Contrary to $\mathbf{M_1}$, $\mathbf{M_2}$ crystallizes in a polar space group. The long chain substituent (hydroxy) can probably induce the noncentrosymmetric packing of chromophores, as was already pointed out in 4-methylthio-4′-(3-sulfonatopropyl)stilbazolium monohydrate.[39] Although dipole-dipole interactions lead to a quasi cancellation of the nonlinearity in the solid state, the structure proves that the hydroxy substituent can be used for promoting acentric alignments of chromophores through hydrogen-bonded networks.[40–43] This strategy, which has already been successfully used by Bosshard and coworkers,[19] appears to be promising. In addition, this substituent might be used for providing opportunities to bond covalently the chromophores into polymers.[44,45] Both approaches offer new challenges for engineering NLO materials with optimal SHG efficiencies.

References

1 See the special issue entitled 'Optical Nonlinearities in Chemistry', *Chem. Rev.*, 1994, **94**(1).
2 P. N. Prasad and D. J. Williams, *Introduction to Nonlinear Optical Effects in Molecules and Polymers*, Wiley-Interscience, New York, 1991.
3 *Materials for Nonlinear Optics: Chemical Perspectives*, ed. S. R. Marder, J. E. Sohn and G. D. Stucky, ACS Symposium Series 455, American Chemical Society, Washington, DC, 1991.
4 J. Zyss, *Molecular Nonlinear Optics*, Academic Press, New York, 1994.
5 D. J. Williams, *Angew. Chem., Int. Ed. Engl.*, 1984, **23**, 690.
6 S. R. Marder, D. N. Beratan and L. T. Cheng, *Science*, 1991, **252**, 103.
7 (*a*) D. R. Kanis, T. J. Marks and M. A. Ratner, *Int. J. Quant. Chem.*, 1992, **43**, 61; (*b*) D. R. Kanis, M. A. Ratner and T. J. Marks, *Chem. Rev.*, 1994, **94**, 195.
8 (*a*) L. T. Cheng, W. Tam, S. H. Stevenson, G. R. Meredith, G. Rikken and S. R. Marder, *J. Phys. Chem.*, 1991, **95**, 10631; (*b*) L. T. Cheng, W. Tam, S. R. Marder, A. E. Stiegman, G. Rikken and C. W. Spangler, *J. Phys. Chem.*, 1991, **95**, 10643.
9 Among recent reports see, for example: (*a*) M. Blanchard-Desce, V. Alain, P. V. Bedworth, S. R. Marder, A. Fort, C. Runser, M. Barzoukas, S. Lebus and R. Wortmann, *Chem. Eur. J.*, 1997, **3**, 1091; (*b*) S. M. LeCours, H.-W. Guan, S. G. DiMagno, C. H. Wang and M. J. Therien, *J. Am. Chem. Soc.*, 1996, **118**, 1497; (*c*) R. V. P. Rao, A. K.-Y. Jen, J. Chandrasekhar, I. N. N. Namboothiri and A. Rathna, *J. Am. Chem. Soc.*, 1996, **118**, 12443; (*d*) L. R. Dalton, A. W. Harper, R. Ghosn, W. H. Steir, M. Ziari, H. Fetterman, Y. Shi, R. V. Mustacich, A. K.-Y. Jen and K. J. Shea, *Chem. Mater.*, 1995, **7**, 1060; (*e*) V. P. Rao, K. Y. Wong, A. K.-Y. Jen and K. J. Drost, *Chem. Mater.*, 1994, **6**, 2210; (*f*) S. Gilmour, R. A. Montgomery, S. R. Marder, L.-T. Cheng, A. K.-Y. Jen, Y. Cai, J. W. Perry and L. R. Dalton, *Chem. Mater.*, 1994, **6**, 1603.
10 C. Flytzanis and A. Dulic, *Opt. Commun.*, 1978, **25**, 402.
11 B. F. Levine, C. G. Bethea, E. Wasserman and L. Leenders, *J. Chem. Phys.*, 1978, **68**, 5042.
12 (*a*) J. Catalan, P. Pérez, J. Elguero and W. Meutermans, *Chem. Ber.*, 1993, **126**, 2445; (*b*) J. Catalan, E. Mena, W. Meutermans and J. Elguero, *J. Phys. Chem.*, 1992, **96**, 3615.
13 J. G. Dawber, S. Etemad and M. A. Beckett, *J. Chem. Soc., Faraday Trans. 1*, 1990, **86**, 3725.
14 P. Jacques, *J. Phys. Chem.*, 1986, **90**, 5535.
15 D. J. A. De Ridder, D. Heijdenrijk, H. Schenk, R. A. Dommisse, G. L. Lemière, J. A. Lepoivre and F. A. Alderweireldt, *Acta Crystallogr. Sect. C*, 1990, **46**, 2197.
16 A. Botrel, A. Le Beuze, P. Jacques and H. Strub, *J. Chem. Soc., Faraday Trans. 2*, 1984, **80**, 1235.
17 A. Klamt, *J. Phys. Chem.*, 1996, **100**, 3349.
18 J. O. Morley, *J. Mol. Struct. THEOCHEM*, 1994, **110**, 191.
19 (*a*) M. S. Wong, F. Pan, C. Bosshard and P. Günter, *Polym. Mater. Sci. Eng.*, 1996, **75**, 132; (*b*) F. Pan, M. S. Wong, V. Gramlich, C. Bosshard and P. Günther, *J. Am. Chem. Soc.*, 1996, **118**, 6315; (*c*) M. S. Wong, F. Pan, V. Gramlich, C. Bosshard and P. Günther, *Adv. Mater.*, 1997, **9**, 554.
20 The synthesis of merocyanine dyes is well-documented. See, for example, I. Gruda and F. Bolduc, *J. Org. Chem.*, 1984, **49**, 3300 and references therein.
21 A. Altomare, G. Cascarano, G. Giacovazzo, A. Guagliardi, M. C. Burla, G. Polidori and M. Camalli, *J. Appl. Crystallogr.*, 1994, **27**, 435.
22 E. Prince, *Mathematical Techniques in Crystallography*, Springer-Verlag, Berlin, 1982.
23 D. J. Watkin, C. K. Prout, J. R. Carruthers and P. W. Betteridge, *Crystals*, Chemical Crystallography Laboratory, University of Oxford, Oxford, 1996, iss. 10.
24 D. J. Watkin, C. K. Prout and L. J. Pearce, *CAMERON*, Chemical Crystallography Laboratory, University of Oxford, Oxford, 1996.
25 (*a*) M. Zerner, G. Loew, R. Kirchner and U. Mueller-Westerhoff, *J. Am. Chem. Soc.*, 1980, **102**, 589; (*b*) W. P. Anderson, D. Edwards and M. C. Zerner, *Inorg. Chem.*, 1986, **25**, 2728.
26 J. F. Ward, *Rev. Mod. Phys.*, 1965, **37**, 1.
27 M. Orchin and H. H. Jaffé, *Symmetry Orbitals and Spectra*, John Wiley, New York, 1971, p. 204.
28 E. Buncen and S. Rajagopal, *Acc. Chem. Res.*, 1990, **23**, 226.
29 M. S. Paley, J. M. Harris, H. Looser, J. C. Baumert, G. C. Bjorklund, D. Jundt and R. J. Twieg, *J. Org. Chem.*, 1989, **54**, 3774.
30 C. Reichardt and E. Harbrush-Görnet, *Liebigs Ann. Chem.*, 1983, **5**, 721.
31 S. Di Bella, I. Fragalà, I. Ledoux and T. J. Marks, *J. Am. Chem. Soc.*, 1995, **117**, 9481.
32 J. Yu and M. C. Zerner, *J. Chem. Phys.*, 1994, **100**, 7487.
33 J. N. Woodford, M. A. Pauley and C. H. Wang, *J. Phys. Chem. A*, 1997, **101**, 1989.
34 C. Dehu, F. Meyers, E. Hendrickx, K. Clays, A. Persoons, S. R. Marder and J. L. Brédas, *J. Am. Chem. Soc.*, 1995, **117**, 10127.
35 (*a*) S. Di Bella, I. Fragalà, M. A. Ratner and T. J. Marks, *Chem. Mater.*, 1995, **7**, 400; (*b*) S. Di Bella, T. J. Marks and M. A. Ratner, *J. Am. Chem. Soc.*, 1994, **116**, 4440; (*c*) S. Di Bella, M. A. Ratner and T. J. Marks, *J. Am. Chem. Soc.*, 1992, **114**, 5842.
36 One referee pointed out that vibrational hyperpolarizability can be very large in donor-acceptor conjugated systems. See for example: B. Kirtman and B. Champagne, *Int. Rev. Phys. Chem.*, 1997, **16**, 389. Intermolecular Interactions are also expected to modify the vibrational NLO response.
37 (*a*) J. L. Oudar and J. Chemla, *J. Chem. Phys.*, 1977, **66**, 2664; (*b*) J. L. Oudar, *J. Chem. Phys.*, 1977, **67**, 446.
38 S. K. Kurtz and T. T. Perry, *J. Appl. Phys.*, 1968, **39**, 3798.
39 (*a*) C. Serbutoviez, J. F. Nicoud, J. Fischer, I. Ledoux and J. Zyss, *Chem. Mater.*, 1994, **6**, 1358; (*b*) I. Gautier-Luneau, C. Serbutoviez and J. F. Nicoud, *Z. Kristallogr.*, 1994, **209**, 531.
40 J. Zyss, R. Masse, M. Bagiue-Beucher and J. P. Levy, *Adv. Mater.*, 1993, **5**, 120.
41 J. Fuller, R. T. Carlin, L. J. Simpson and T. E. Furtak, *Chem. Mater.*, 1995, **7**, 909.
42 (*a*) R. Renuka, T. N. Guru Row, B. R. Prasad, C. K. Subramanian and S. Bhattacharya, *New J. Chem.*, 1995, **19**, 83; (*b*) P. Dastidar,

T. N. Guru Row, B. R. Prasad, C. K. Subramanian and S. Bhattacharya, *J. Chem. Soc., Perkin Trans. 2*, 1993, 2419.
43 F. Pan, M. S. Wong, V. Gramlich, C. Bosshard and P. Günter, *J. Chem. Soc., Chem. Commun.*, 1996, 1557.
44 (*a*) C. Xu, B. Wu, M. W. Becker and L. P. Dalton, *Chem. Mater.*, 1993, **5**, 1439; (*b*) C. Xu, B. Wu, L. R. Dalton, Y. Shi, P. M. Ranon and W. H. Steier, *Macromolecules*, 1993, **26**, 5303.
45 (*a*) M. A. Hubbard, T. J. Marks, W. P. Lin and G. K. Wong, *Chem. Mater.*, 1992, **4**, 965; (*b*) J. T. Lin, M. A. Hubbard, T. J. Marks, W. P. Lin and G. K. Wong, *Chem. Mater.*, 1992, **4**, 1148.

Received in Montpellier, France, 22nd January 1998;
Paper 8/00634B